Neuroscience 121 (2003) 573–586

IMMUNOHISTOCHEMICAL LOCALIZATION OF MYOSIN Va IN THE ADULT RAT BRAIN

C. Q. TILELLI,[a] A. R. MARTINS,[b] R. E. LARSON[c] AND N. GARCIA-CAIRASCO[a]*

[a]*Department of Physiology, Faculdade de Medicina de Ribeirão Preto, Universidade de São Paulo, Av Bandeirantes, 3900, 14049–900 Ribeirão Preto, São Paulo, Brazil*

[b]*Department of Pharmacology, Faculdade de Medicina de Ribeirão Preto, Universidade de São Paulo, 14049–900 Ribeirão Preto, São Paulo, Brazil*

[c]*Department of Cellular and Molecular Biology and Pathogenic Bioagents, Faculdade de Medicina de Ribeirão Preto, Universidade de São Paulo, 14049–900 Ribeirão Preto, São Paulo, Brazil*

Abstract—Brain myosin Va (MVa) is a molecular motor associated with plastic changes during development. MVa has previously been detected in the cell body and in dendrites of neuronal cells in culture, in cells of the guinea-pig cochlea, as well as in cerebellar cells. Adult Wistar rats (n=14), 250–300 g, were perfused with standard methods for immunohistochemistry, using a polyclonal, affinity-purified rabbit antibody against MVa tail domain. Anti-MVa antibody specifically stained neuronal nuclei from forebrain to cerebellar regions, and more intensely sensory nuclei. Differences in MVa immunoreactivity were detected between brain nuclei, ranging from very intense to weak staining. The analysis of MVa and glial fibrillary acidic protein staining in adjacent brain sections demonstrated a clear-cut neuronal labeling rather than an astroglial staining. The studies presented here represent a comprehensive map of MVa regional distribution in the CNS of the adult rat and may contribute to the basic understanding of its role in brain function and plasticity, particularly in relationship to phenomena that involve molecular motors, such as neurite outgrowth, organelle transport and neurotransmitter-vesicle cycling. It is important to highlight that this is a pioneer immunohistochemical study on the distribution of MVa on the whole brain of adult rats, a first step toward the understanding of its function in the CNS.

Key words: MVa, molecular motor, cytoskeleton, neuroanatomical mapping, plasticity.

Myosin Va (MVa) is a molecular motor, involved in actin-based cellular motility, that features a well-conserved, mechanochemical head domain, an elongated neck domain composed of six tandem repeats of the IQ motif and a distinct tail domain that includes coiled-coil and globular regions. The class V myosins have been implicated in organelle and RNA transport in several organisms (for review see Reck-Peterson et al., 2000). Mammalian brain is a rich source of MVa, from which it has been purified and biochemically characterized (Espíndola et al., 1992; Espreafico et al., 1992; Cheney et al., 1993; Nascimento et al., 1996; Tauhata et al., 2001). The expression of MVa is deficient in *dilute* mice (Mercer et al., 1991) and *dilute-opisthotonus* rats (Futaki et al., 2000), both of which present seizures soon after birth and die within the third post-natal week. The specific dysfunction that leads to the convulsions and post-natal death in these animals is not known. However, recent evidence has implicated MVa in several neuronal processes, including its binding to synaptic vesicle associated proteins (Prekeris and Terrian, 1997; Costa et al., 1999; Ohyama et al., 2001), its association with organelle and vesicle movement within axons (Evans et al., 1998; Tabb et al., 1998) as well as its critical role in the localization of smooth endoplasmic reticulum in dendritic spines of Purkinje cells (Dekker-Ohno et al., 1996). The subcellular localization of MVa has been described in neuronal and glial cells by immunoprobes and shows a characteristic punctate labeling, frequently being concentrated at the neurite tips and growth cones, as well as at the perinuclear region (Espreafico et al., 1992).

MVa is broadly distributed in many brain regions in the mouse (Mercer et al., 1991) although strikingly intense labeling has been reported in specific cell types, such as Purkinje cells of the cerebellum (Espíndola et al., 1992; Espreafico et al., 1992), the outer plexiform layer of the retina (Schlamp and Williams, 1996) and a subset of neurons in the myenteric ganglia (Drengk et al., 2000).

In the present study, we have used affinity-purified antibodies against MVa to delineate its expression in the brain of the adult rat. The immunohistochemical studies presented here represent a comprehensive map of MVa regional distribution in the CNS of the adult rat and may contribute to the basic understanding of its role in brain function and plasticity, particularly in relationship to phenomena that involve molecular motors, such as neurite outgrowth, organelle transport and neurotransmitter-vesicle cycling.

EXPERIMENTAL PROCEDURES

Animals

Fourteen male albino Wistar rats weighing 250–350 g were given water and food *ad libitum* and maintained under optimal temper-

*Corresponding author. Tel: +55-16-602-3330; fax: +55-16-633-0017.
E-mail address: ngcairas@fmrp.usp.br (N. Garcia-Cairasco).

Abbreviations: DEn, endopiriform nucleus; EDTA, ethylenediaminetetraacetic acid; Fr1, frontal cortex, area 1; Fr2, frontal cortex, area 2; GFAP, glial fibrillary acidic protein; IC, inferior colliculus; LaDL, lateral amygdaloid nucleus, dorsolateral area; LaVL, lateral amygdaloid nucleus, ventrolateral area; Me5, mesencephalic trigeminal nucleus; MVa, myosin Va; NARF, neural activity-related RING finger protein; NF, neurofilament; PBS, 20 mM sodium phosphate buffer, pH 7.4, containing 150 mM NaCl; SDS-PAGE, sodium dodecyl sulfate–polyacrylamide gel electrophoresis.

0306-4522/03$30.00+0.00
doi:10.1016/S0306-4522(03)00546-3

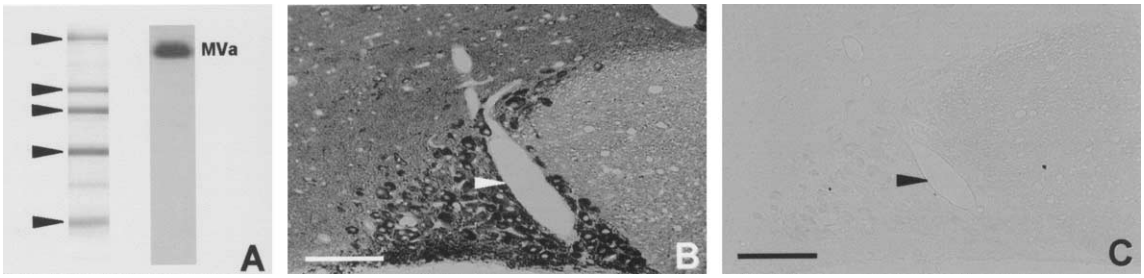

Fig. 1. Immunological specificity of the MVa antibody detected by chemoluminescence (A), after a Western blot assay. Left lane: Molecular weight markers 205, 116, 97, 66 and 45 kD. Right lane: MVa (190 kD). Immunohistochemical staining of the supraoptic nucleus with MVa (B) and suppression with the pre-adsorbed MVa antibody (C). The area showed in B and C is the same in adjacent sections (arrows). Calibration bars=100 μm.

ature and humidity conditions, with a 12-h light/dark cycle (lights on at 7:00 h and lights off at 19:00 h). Experiments on laboratory animals were conducted in accordance with the rules of the Brazilian Society for Neuroscience and Behavior, which are based on the Society for Neuroscience guidelines for animal experimentation. All efforts were made in order to avoid any unnecessary suffering or pain to the animals.

Tissue processing and immunohistochemistry

Each rat was anesthetized with sodium thionembutal (Abbott Laboratórios do Brasil LTDA, São Paulo, Brazil; 45 mg/kg, ip) and perfused transcardially with 4% (wt/vol) paraformaldehyde in 100 mM sodium phosphate, pH 7.4. Brains were removed and consecutive brain sections (3 mm each) were then cut at sagittal or coronal planes. These sections were further immersion-fixed for 2 h in the same fixative. Fixed tissues were dehydrated in ethanol, cleared in xylene and embedded in paraffin. Six micrometer sections were cut and mounted on gelatin-chrome aluminum-coated microscope slides.

MVa expression was detected using affinity-purified, polyclonal antibody, generated in rabbits inoculated with de bacterially expressed tail domain of MVa, initially characterized by Espreafico et al. (1992). The detection of MVa in tissue sections after antigen retrieval using 10 mM citrate buffer, pH 6, was performed according to Martins et al. (1999). Thereafter, sections were incubated with H_2O_2 in 20 mM sodium phosphate buffer, pH 7.4, containing 150 mM NaCl (PBS) for 15 min, followed by a 4 h incubation in 0.02 M sodium phosphate buffer, pH 7.4, containing 450 mM NaCl and 0.2% (w/v) Triton X-100 (New England Nuclear, Boston, MA, USA; Triton buffer), and 15% (v/v) normal goat serum (blocking buffer), for 4 h. Sections were incubated overnight with anti-MVa (50 μg/ml) in blocking buffer and washed with Triton buffer after each incubation. Endogenous biotin was blocked using a biotin blocking system (Dako, Glostrup, Denmark). Sections were then incubated for 30 min with biotinylated swine anti-rabbit IgG diluted 1:200 in blocking buffer (Dako). The biotinylated second antibody was detected using the ABC technique (Elite ABC kit; Vector Laboratories, Burlingame, CA, USA) and diaminobenzidine (Pierce, Rockford, IL, USA) as the chromogen. All operations were carried out at room temperature. Sections were mounted with Permount (Fischer, Springfield, NJ, USA) and analyzed using an Olympus BX60 microscope. Controls included the substitution of primary antibodies with serum from non-inoculated rabbits and the preadsorption of anti-MVa antibodies with MVa protein.

Essentially the same immunohistochemical procedure, except for exchanging of the primary and secondary antibodies, was used to detect other proteins, such as neurofilament (anti-NF; Dako) and glial fibrillary acidic protein (anti-GFAP; Dako). Additionally, Nissl staining (Cresyl Violet) was used for tissue histochemistry.

The regions of the rat brain were identified using the Atlas by Paxinos and Watson (1997).

Image Acquisition

Images were acquired using a cold-CCD 750L digital camera (Optronics, Goleta, CA, USA) and the Neurolucida 2000 (MicroBrightField, Williston, VT, USA) software. All images were acquired with the same characteristics of brightness and contrast.

Gel electrophoresis and immunoblotting

Rats were killed by decapitation, and their brains were quickly dissected. Brains were homogenized in 25 mM Tris–HCl buffer, pH 8.5, containing 10 mM EDTA, 5 mM ATP, 2 mM β-mercaptoethanol, 0.3 mM phenylmethylsulfonylfluoride, 1 mM benzamidine and 3 μM aprotinin. A supernatant fraction (10 mg protein/ml), obtained by centrifugation of the homogenate at 14,000×*g*×30 min, was diluted five-fold with 0.26 M Tris–HCl buffer, pH 6.8, containing 7.3% (w/v) sodium dodecyl sulfate, 16.6% (w/v) sucrose, 3.5 M β-mercaptoethanol and 0.005% (w/v) Bromophenol Blue, and boiled for 3 min. The material was used immediately for sodium dodecyl sulfate–polyacrylamide gel electrophoresis (SDS-PAGE) and Western blotting.

SDS-PAGE was carried out in 7–15% gradient minigels, using a discontinuous system (Laemmli and Favre, 1973). Western blotting to nitrocellulose membranes (Hybond-C extra from Amersham, Buckinghamshire, UK) was performed according to Towbin et al. (1979). The specificity of the anti-MVa antibody was determined by immunoblot analysis of homogenates from rat brain. The immunoblots were developed by an enhanced chemiluminescence procedure as described by the manufacturer (Amersham), using Hyperfilm ECL (Amersham). Molecular mass standards used were: rabbit muscle myosin, 205 kDa; *E. coli* β-galactosidase, 116 kDa; rabbit muscle phosphorylase B, 97 kDa; bovine serum albumin, 66 kDa; egg albumin, 45 kDa (Sigma, St. Louis, MO, USA).

Protein determination

Protein concentration was determined by the method of Lowry et al. (1951), with bovine serum albumin as the standard.

RESULTS

Specificity of the MVa immunohistochemical assay

Affinity purified polyclonal antibodies raised against the tail domain of chicken brain MVa recognized a single 190 kDa band on Western blots of rat brain homogenates (Fig. 1A), in agreement with the molecular mass of this protein. The specificity of these antibodies for the

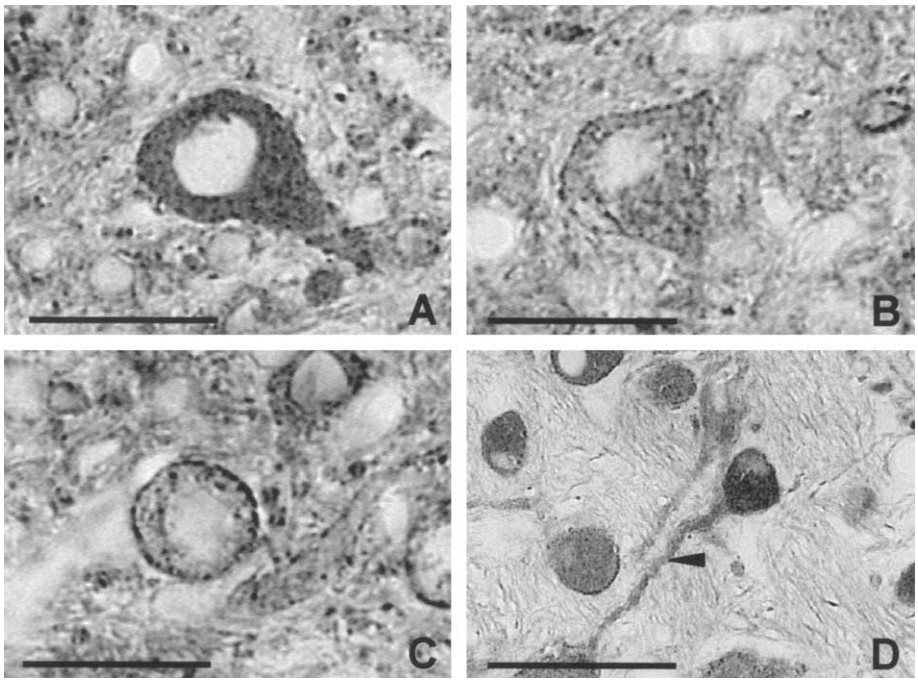

Fig. 2. Different MVa immunohistochemical staining patterns were observed in several regions of the rat brain. Independent of the staining pattern presented, it was always cytoplasmic, and no labeling of the cell nucleus was ever detected. The staining was also either strong or weak, but exhibited different patterns, such as: (A) densely punctate staining, ventral cochlear nucleus; (B) sparse punctate staining, dorsal cochlear nucleus; (C) peripheral punctate staining, dorsal cochlear nucleus; (D) cell processes staining (arrow), ventral cochlear nucleus. Calibration bars=25 μm in A–C; 50 μm in D.

MVa paralogue was confirmed by their lack of labeling on Western blots of brain homogenates from homozygous *dilute lethal* mice (unpublished data), which are null for MVa. An immunohistochemical control fraction was generated from the MVa antibody by preadsorption with MVa protein. This control fraction did not stain MVa on Western blots of a rat brain homogenate (not shown) nor in tissue sections, as in this example, of the supraoptic nucleus (Compare Fig. 1B and C).

Immunoreactivity of MVa in cells and brain regions

The immunolabeling of MVa was detected in many regions of adult rat brain, ranging from brainstem and cerebellum to forebrain. At higher magnifications labeling was detected both in neuronal cell bodies (Fig. 2A–C) and their processes (Fig. 2D). Although not all the neurons in a given region showed staining, those displaying immunolabeling did present a diversity of patterns, which we describe here as densely punctate (Fig. 2A), sparsely punctate (Fig. 2B) and peripherally punctate (Fig. 2C). Intermediate intensities of staining were also encountered. MVa was not detected in astroglia, which were, however, conspicuously labeled by the anti-GFAP antibody (Fig. 3).

In order to examine the immunohistological localization of MVa in specific brain regions we compared adjacent tissue slices of the trapezoid body, the cerebellum and the hippocampus by staining with Cresyl Violet (Nissl) or labeling with antibodies against NF protein, GFAP or MVa (Fig. 4). Strong immunoreactivity for MVa was observed in neuronal cell bodies within the nucleus of the trapezoid body, as well as more subdued, yet clearly obvious, labeling of fibers in the trapezoid body itself (Fig. 4A). This result is accentuated by comparing the images obtained from the adjacent tissue slices: intense staining of NF protein in fibers and cell bodies of neurons (Fig. 4D); intense GFAP staining of glial cells, but only background levels of staining in fibers (Fig. 4G); and Nissl staining of cell bodies delineating the nucleus of the trapezoid body (Fig. 4J).

The cerebellum shows uniform labeling of MVa in the molecular layer as well as more tenuous, but clear, labeling of the granular layer (Fig. 4B). In contrast, little or no immunoreactivity for MVa was observed in the bulk of white matter of the cerebellum. In contrast, note that the NF antibodies labeled strongly these fibers (Fig. 4E). Observe also the clear labeling of cell bodies in the Nissl staining (Fig. 4K).

By comparison, the hippocampus was more uniformly labeled by the MVa antibodies, showing less contrast between intrahippocampal structures than the previous two regions described (Fig. 4C), although the staining by anti-MVa of cell bodies in subiculum (Fig. 6C) and in the dentate gyrus (Fig. 6B) was quite prominent under greater magnification. In contrast, labeled structures within the hippocampus are clearly seen with the other markers such as Nissl (Fig. 4L). In addition to that, hippocampal fibers (e.g. fimbria-fornix) are well defined with the NF staining (Fig. 4F) and the hilus and external molecular layer are evident with GFAP staining (Fig. 4I).

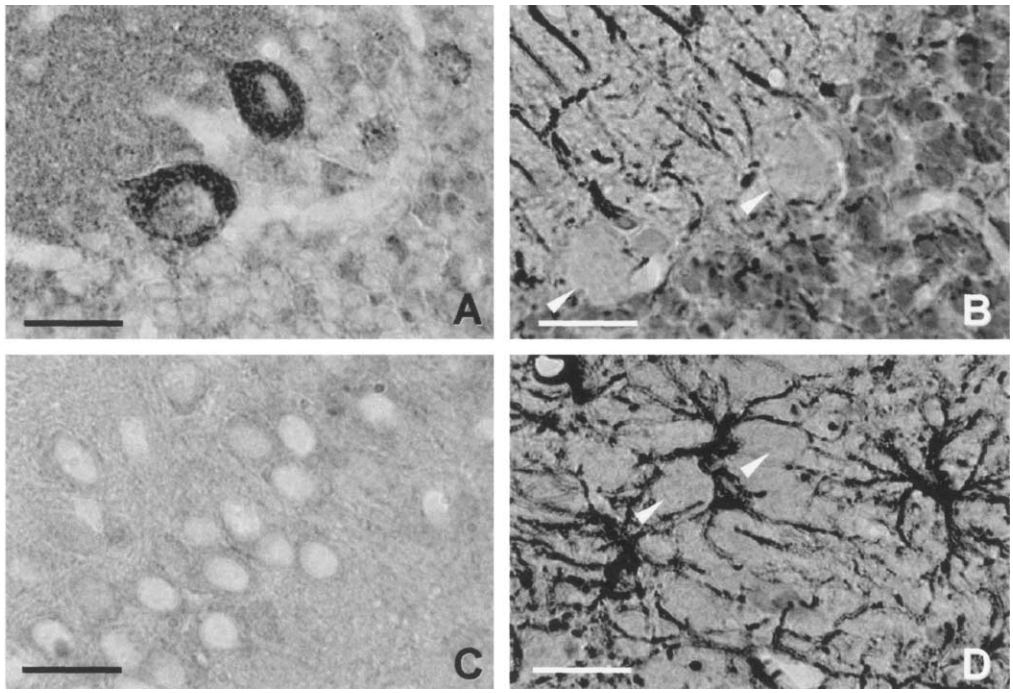

Fig. 3. Comparison of MVa stained areas (A and C) with adjacent sections immunohistochemically stained with anti-GFAP antibody (B and D). Note that MVa does not stain cells in a pattern found in astroglia. A, B: Cerebellar cortex, Purkinje cell layer; C, D: Ammon's Horn, area 1. Arrows in B and D indicate negative GFAP staining of cells that labeled positively for MVa in A and C. Calibration bars=20 μm.

There was no evidence for the staining of glial cells by the MVa antibody in any of the three regions analyzed (also see Fig. 3).

Regional analysis of MVa expression

In Figs. 5–9, different regions and cells of the brain showing immunoreactivity for MVa are described in detail, using as anatomical reference the coordinates and nomenclature (see Table 1) taken from the stereotaxic atlas of Paxinos and Watson (1997). In each of the following figures, it will be shown a sequence of a sagittal image (inset), indicating the stereotaxic atlas level (using as the reference distance from bregma suture in millimeters), followed by a coronal section, with labeled structures zoomed in were precise descriptions were done. The general description was from rostral to caudal regions. It is clear that not all the cell populations were described or indicated in the figures, but those where we felt the more conspicuous patterns were found. Table 2 highlights a summary of the MVa staining patterns in different brain areas, which will be described in detail in the following paragraphs.

At Bregma 0.70 mm (Fig. 5A)

Punctate immunostaining was observed in the indusium griseum (Fig. 5B), mostly in the dorsomedial region, and in the cingulate cortex, areas 1 (Fig. 5C), 2 and 3, around cell bodies and fibers. Some of the deep cortical layers presented a dense cytoplasmic staining of the cell that was not found in more superficial cortical layers, although all cortical layers were stained. Some of the divisions of the cortex—frontal cortex 1 (Fr1; Fig. 5D) and frontal cortex 2 (Fr2), forelimb area of cortex and area 1 of parietal cortex—presented a sparse punctate staining in the cell body. A similar pattern was observed in the granular insular cortex. Claustrum, dorsal endopiriform nucleus (DEn), dysgranular insular cortex and agranular insular cortex had a characteristic punctate staining of the cell body. In the external layer of piriform cortex (Fig. 5E, arrowheads), there was a dense punctate staining and, more deeply, sparse cell body staining. In the ventral pallidum, we also found an intermediate punctate labeling in cells and in some cell processes. The cell bodies of medial septal nucleus were peripherally punctated. In the habenular nucleus we found sparse staining in lateromedial and anterolateral areas, and a denser one in the medial area. Cells of diagonal band (Fig. 5F) were intermediately punctated. The intermediate part of the lateral septal nucleus presented exclusively peripheral punctate staining. The MVa staining was absent in the lateral septal nucleus and caudate putamen.

At Bregma −3.30 mm (Fig. 6A)

The retrosplenial granular cortex presented a peripheral staining of both cell bodies and processes in layers 1–3. Layers 4–6 presented cell body staining. In the retrosplenial agranular cortex, we found a mixed staining, denser in some cells. Fr1, Fr2 and hindlimb area of cortex presented staining in cell bodies from layers 4–6. Both areas 1 and 2 of parietal cortex presented a sparse staining of cell bodies in layers 1–3, and a denser staining in layers 4–6. In the

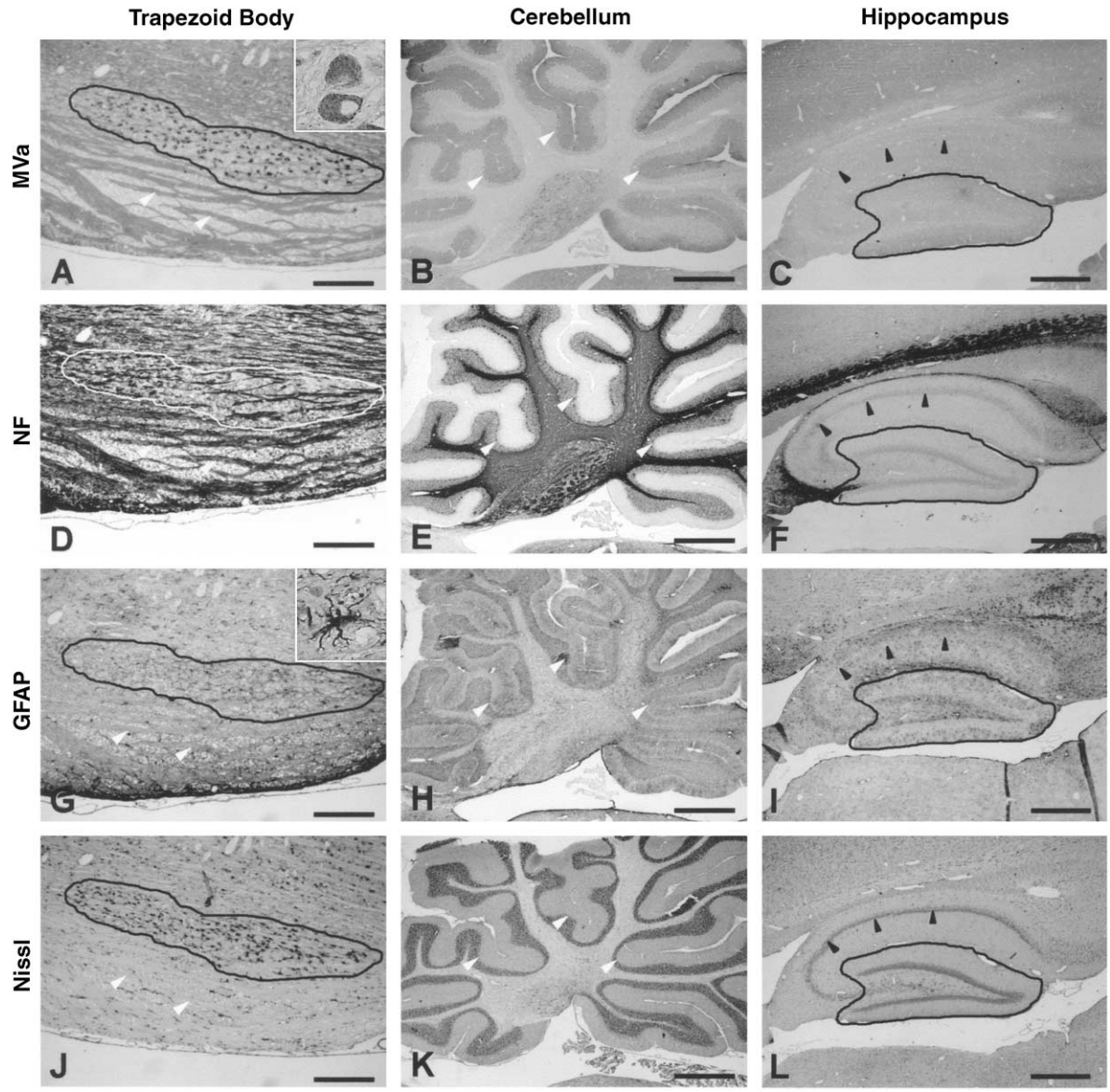

Fig. 4. Adjacent sagittal rat brain sections labeled with MVa (A–C), NF (D–F), GFAP (G–I) and Nissl (J–L) at the level of trapezoid body (left), cerebellum (center) and hippocampus (right). Calibration bars=250 μm (trapezoid body); 750 μm (cerebellum) and 500 μm (hippocampus). In the trapezoid body images, outline indicates the nucleus of the trapezoid body and arrows indicate the trapezoid body itself (fibers). In the cerebellum images, arrows indicate the cerebellar cortex. In the hippocampal formation images, arrows indicate Ammon's horn and outline indicates dentate gyrus. See details in text.

perirhinal cortex, we found densely stained cell bodies in layers 4–6 and, although similar staining was found in superior layers, there was no good delimitation of cells. In the DEn the cells presented a very sparse staining intermixed with the neuropila. The lateral amygdaloid nucleus presented a sparse punctate staining in the dorsolateral (LaDL) and ventrolateral (LaVL) areas, and a very sparse punctate staining of ventromedial area, similar to the DEn. The anterior and posterior parts of basolateral amygdaloid nucleus presented a staining similar to the one described for LaDL and LaVL. In the medial amygdaloid nucleus as well as in the posterodorsal area, we found a strong peripheral staining of the cell body. Additionally, we found some cell bodies stained in the posteroventral area. The same kind of peripheral cell staining was found in the dorsomedial hypothalamic nucleus. MVa was almost absent in hippocampal dentate granular cells, but some hilar neurons were stained (arrows; Fig. 6B). Isolated Ammon's horn cells were found densely stained in areas 1, 2 and 3, when compared with a predominant weak staining found in pyramidal neurons of the same areas. In the subiculum the cell body staining was dense (Fig. 6C). A dense staining of cell bodies was also found in ventral posterolateral (Fig. 6D) and medial thalamic nuclei (Fig. 6E). A sparser staining was found in cell bodies of mediodorsal thalamic nucleus, lateral, central and medial areas, and in posterior

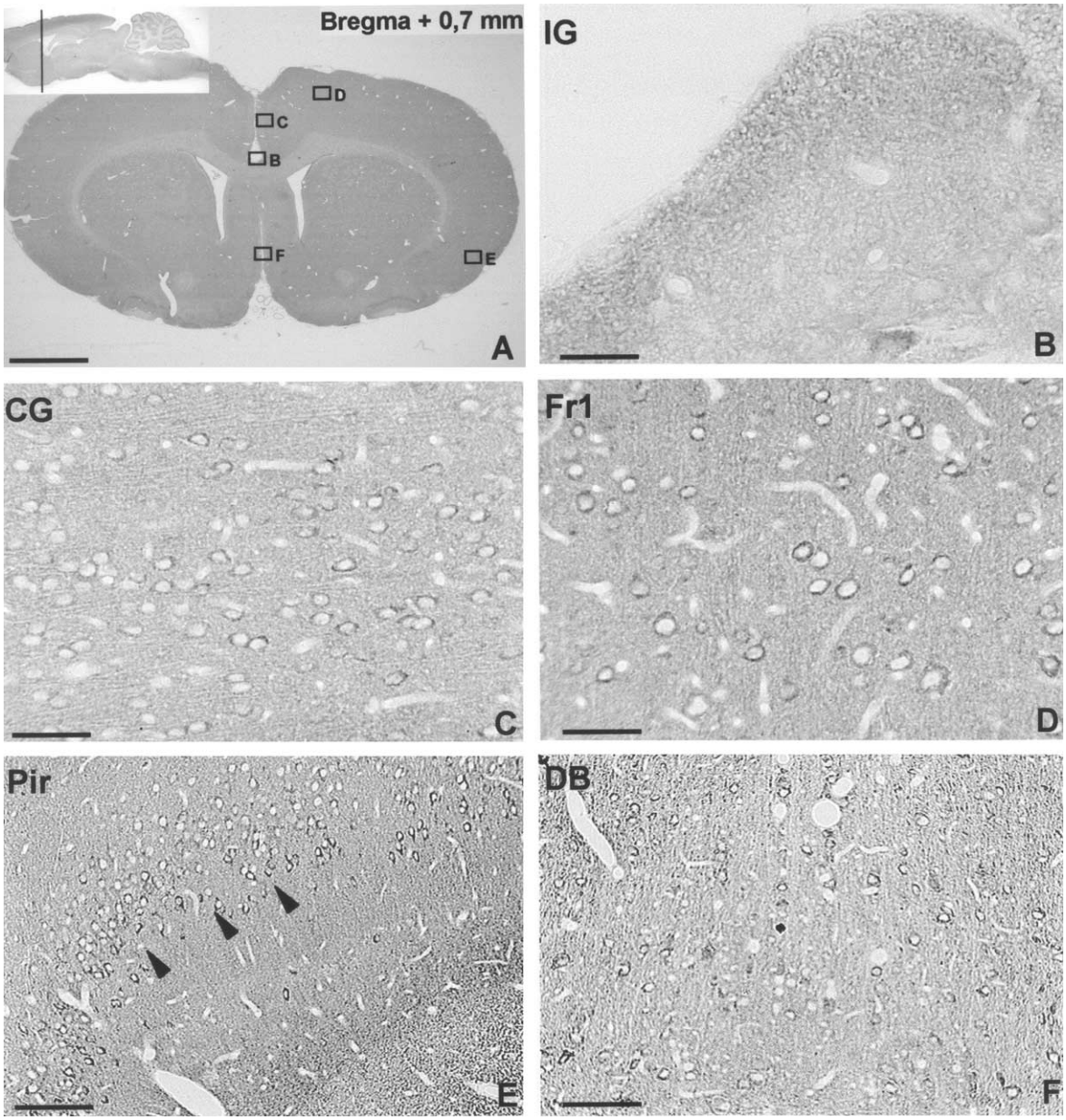

Fig. 5. A. Panoramic coronal view of a rat brain, at the level of striatum and septal area, immunolabeled with anti-MVa antibody. B–F. Higher magnifications of regions corresponding to lettered rectangles in A. Calibration bars=1000 μm for A, 25 μm for B, 50 μm for C and D, 100 μm for E and F. See details in text.

paraventricular thalamic nucleus. There were cell bodies densely stained in the median eminence (Fig. 6F), and more sparsely in perifornical nucleus, medial tuberal nucleus, magnocellular nucleus of lateral hypothalamus, subincertal nucleus, zona incerta, posterior thalamic nuclear group, laterodorsal thalamic nucleus (dorsomedial and ventrolateral areas) and lateral posterior thalamic nucleus, mediodorsal area.

Bregma −5.8 mm (Fig. 7A)

The cortical areas presented the same staining pattern described in previous sections. In the zonal layer of superior colliculus, the cell bodies and neuropila were densely stained. In the superior colliculus there were cell bodies with variable staining, in the superficial gray layer, as well as in the optic nerve layer, intermediate gray layer and intermediate white layer. In the posterior pretectal nucleus (Fig. 7B), large cell bodies were densely stained, and in medial geniculate nucleus (Fig. 7C) there was a similar staining for large and small cells. A peripheral punctate staining was found in the ventral part of this nucleus. In the deep mesencephalic nucleus we found some densely stained cells. In the substantia nigra (Fig. 7D) the staining was dense, but the neuropila

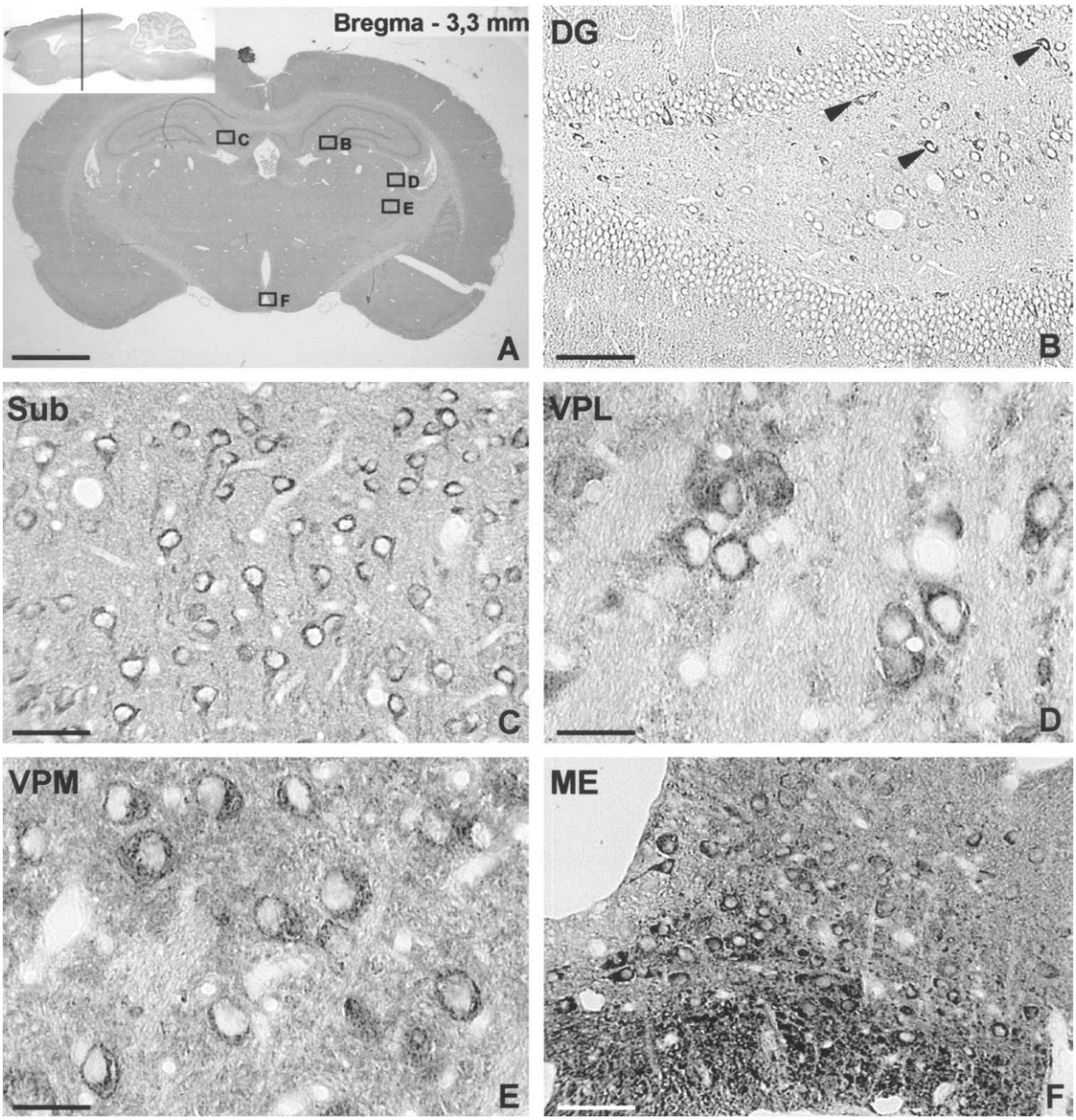

Fig. 6. A. Panoramic coronal view of a rat brain, at the level of the dorsal hippocampus and anterior thalamus, immunolabeled with anti-MVa antibody. B–F. Higher magnifications of regions corresponding to lettered rectangles in A. Calibration bars=1000 μm for A, 100 μm for B; 25 μm for C and D; 50 μm for E and F. See details in text.

was very sparsely labeled in pars compacta and in pars lateralis, when compared with pars reticulata. The staining was very dense in cells and in neuropila, in the interpeduncular nucleus. In the red nucleus (Fig. 7E), as well as in the Edinger-Westphal nucleus, cell bodies were densely punctated. Cell bodies with very peripheral staining were found in central gray. In the mesencephalic trigeminal nucleus (Me5; Fig. 7F) we found both dense (white arrowhead) and peripheral (black arrowhead) cell body staining.

Bregma −7.8 mm (Fig. 8A)

The cortical areas presented the same staining pattern described in previous sections. Cells in the periolivary nucleus (Fig. 8B) were densely stained, and the adjacent neuropila was strongly stained. There were conspicuously stained cells in all inferior colliculus (IC) nuclei, particularly in the external cortex of IC (Fig. 8C). A peripheral staining of cell bodies was also found in the commissure of the IC. Median raphe nucleus (Fig. 8D) presented densely and sparsely punctated cell body staining. A dense labeling was found in cell bodies of pontine nuclei, oral pontine reticular nucleus (Fig. 8E), median raphe nucleus, paramedian raphe and lateral lemniscus (Fig. 8F). In the cuneiform nucleus, we found dense and peripheral staining of cells.

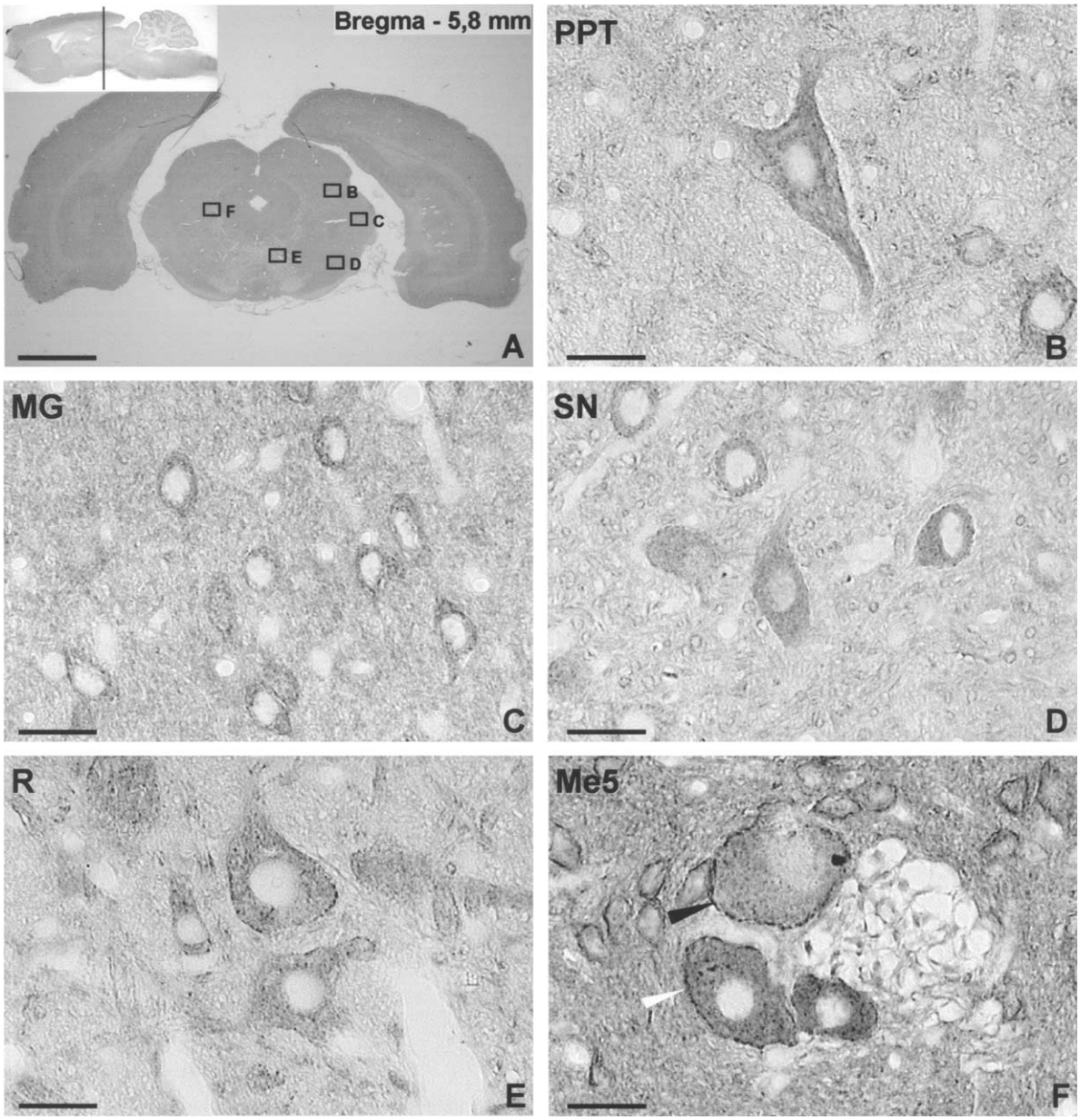

Fig. 7. A. Panoramic coronal view of a rat brain, at the level of superior colliculus and substantia nigra, immunolabeled with anti-MVa antibody. B–F. Higher magnifications of regions corresponding to lettered rectangles in A. Calibration bars=1000 μm for A, 25 μm for B–F. Observe in F, at the level of the Me5, simultaneous peripheral (black arrow) and intermediate punctate (white arrow) staining. See details in the text.

Bregma −11.30 mm (Fig. 9A)

Cells of the raphe magnus nucleus (Fig. 9B) and the oral part of the spinal trigeminal nucleus were densely punctated. In medial vestibular nucleus (Fig. 9C), prepositus hypoglossal nucleus, interposed cerebellar nucleus and vestibular nucleus, we found cell body staining and peripheral cell staining, but with a sparser neuropila staining of the latter. In the cerebellar cortex (Fig. 9D), both soma and dendrites of Purkinje cells (small black arrows) and granular cells (white arrow) were densely stained. The entire molecular layer showed also considerable staining indicating labeling of the dendritic tree of the Purkinje cells and/or parallel fibers (big black arrow). The cochlear nucleus presented a very dense staining, with its dorsal part (Fig. 9E) presenting peripheral cell staining more laterodorsally and dense cell body staining more ventromedially, and its ventral part (Fig. 9F) with a combination of numerous densely punctate cell bodies staining and some peripheral cell staining.

DISCUSSION

Myosin-V represents a class of molecular motors implicated in organelle and RNA transport in several organisms. Its association in brain with nerve terminals (Mani et al., 1994; Prekeris and Terrian, 1997), synaptic vesicles

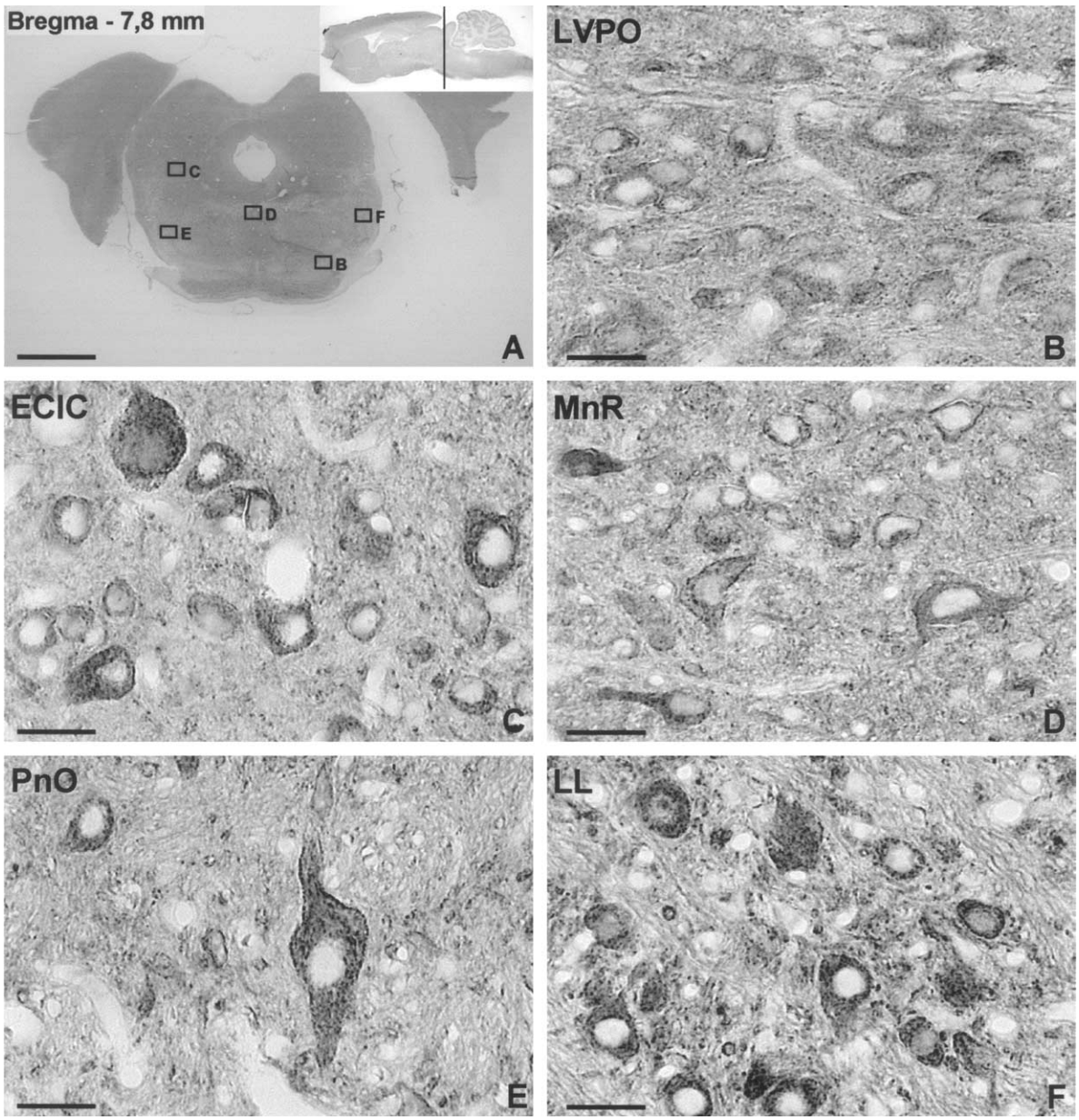

Fig. 8. A. Panoramic coronal view of a rat brain, at the level of IC and pontine nuclei, immunolabeled with anti-BM-V antibody. B–F. Higher magnifications of regions corresponding to lettered rectangles in A. Calibration bars=1000 μm for A, 25 μm for B–F. See details in the text.

and synaptic vesicle associated proteins (Prekeris and Terrian, 1997; Costa et.al., 1999; Ohyama et al., 2001) as well as with organelle movement in axons (Evans et al., 1998; Tabb et al., 1998) suggest that myosin V has a functional role in organelle transport.

The characteristic punctate labeling of MVa in virtually all neural cells examined to date is in accordance with this function in vertebrate nervous system (Espreafico et al., 1992). The exact role of MVa at the synapse has not been determined, but suggestions have been made that this molecular motor may be involved in transport of synaptic vesicles from reserve pools toward the active zone where membrane fusion and neurotransmitter release occur (Costa et al., 1999; Rosé et al., 2003).

The expression of MVa is deficient in *dilute* mice (Mercer et al., 1991) and *dilute-opisthotonus* rats (Futaki et al., 2000). Both mutants present post-natal seizures and die within 3 weeks after birth. No specific neurological dysfunction has been determined that would directly link the convulsions and the post-natal death in these animals. For example, a recent study on synaptic function in hippocampal cells, a region important for the manifestation of epileptic dysfunctions, demonstrated apparently normal synaptic transmission in *dilute* mice, null for MVa (Schnell and Nicoll, 2001). Also, in the immunohistochemical studies presented here, the expression of MVa is not exceptionally high in hippocampal cells as compared with other brain regions. In the adult rat brain MVa is widely expressed in

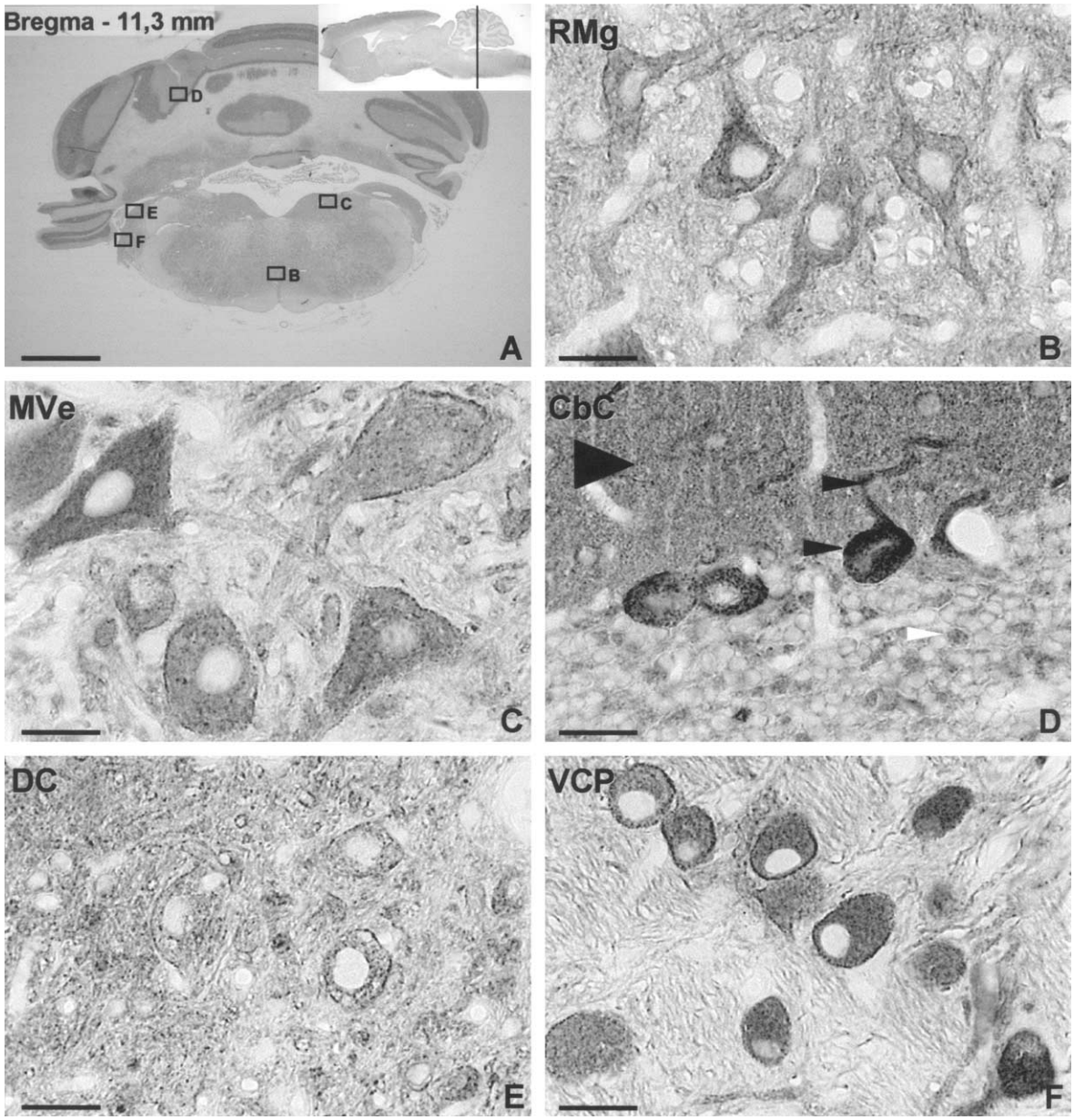

Fig. 9. A. Panoramic coronal view of a rat brain at the level of cerebellum and medulla, immunolabeled with anti-MVa antibody. B–F. Higher magnifications of regions corresponding to lettered rectangles in A. Calibration bars = 1000 μm, 25 μm for B–F. Observe in D at the level of the cerebellar cortex, strong staining of cell dendrites and perikarya (small black arrows) of Purkinje cells. Simultaneously are strongly stained cell bodies of granule cells (white arrow). See other details in the text.

many regions and cellular layers, although both the pattern and intensity of MVa immunoreactivity differed from region to region. On the one hand, structures such as the cochlear nuclei, trapezoid body, superior olivary complex, red nucleus and vestibular nucleus, which are important in sensory processing and sensory-motor integration within the CNS, showed strong immunostaining for MVa in cells and neuropila (see Figs. 4–9). On the other hand, regions that are associated with more complex functions, such as the cortex, hippocampus and amygdala, showed a weaker staining of cells and associated neuropila. However, the subcellular patterns of immunoreactivity for MVa observed in the present study were found in neurons distributed throughout the brain, without being specifically associated to known anatomical or functional regions. In fact, the wide distribution of several cellular-staining patterns, such as dense punctate, peripheral punctate and sparse punctate, was suggestive of specific cell function and cell–cell communication. Thus, the variation in expression of MVa in specific cells or in subcellular locations may be related to cell specific activity.

Our data confirm the intense labeling that has been reported in specific cell types, such as Purkinje cells of the cerebellum (Espíndola et al., 1992; Espreafico et al., 1992). Our results also extend these descriptions to col-

Table 1. Abbreviations used in Figures 5–9

IG, *indusium griseum*
DB, diagonal band
VPL, ventral postero lateral thalamic nucleus
Sub, *subiculum*
PPT, posterior pretectal nucleus
SN, *substantia nigra*
ECIC, external cortex of inferior colliculus
PnO, oral pontine reticular nucleus
RMg, *raphe magnus* nucleus
CbC, cerebelar cortex
VCP, ventral cochlear nucleus
CG, clingulate cortex
Pir, piriform cortex
GD, dentate granular cells
VPM, ventral postero medial thalamic nucleus
ME, median eminence
MG, medial geniculate nucleus
R, red nucleus
LVPO, latero ventral periolivary nucleus
MnR, median *raphe* nucleus
LL, lateral *lemniscus* nucleus
MVe, medial vestibular nucleus
DC, dorsal cochlear nucleus

lections of diverse brain neuroanatomical nuclei confirming that MVa is amply expressed throughout the CNS, indicating a general role in neuron function. However, intense labeling of specific cells and group of cells is also observed, suggesting that MVa may have a punctual expression related to cell activation and/or regional/temporal functions where molecular motors are needed. Furthermore, based on the MVa and GFAP immunolocalization studies, our data do not confirm specific expression of MVa in astroglial cells in contrast to its expression in cultured glial cells (Espreafico et al., 1992). Therefore, our data strongly suggest that MVa is a specific neuronal marker in agreement with others (Langford and Molyneaux, 1998; Hasson et al., 1997; Mooseker and Cheney, 1995).

Although we observed a relatively homogeneous pattern of expression of MVa in a given brain region or nucleus (e.g. cochlear nucleus, nucleus of the trapezoid body) of the animals of the current study, we also observed different intensities (e.g. strong versus weak) in the same region. Furthermore, we found that there are striking differences in the MVa expression when the comparison is made between different brain nuclei (e.g. cochlear nucleus versus granule cells of the hippocampal dentate gyrus). If these variations have any functional meaning, we currently do not know. Obvious experiments need to be done with, for example, *in vitro* preparations such as cell cultures or slices, which together with video-microscopy could address these issues properly.

A detailed analysis of the entire series of sections processed in this study indicates an interesting range of patterns that may be associated with regional networks. An interesting example is the auditory pathway. Hasson et al. (1997) and Coling et al. (1997) described the immunolocalization of MVa in neuronal and supporting cells of the sensory epithelium of the cochlea of the guinea-pig, which is complementary to the conspicuous immunostaining of auditory central nuclei, such as cochlear nucleus, trapezoid nucleus, superior olivary complex and lateral lemniscus nuclei, observed in the present work. Interestingly, MVa strongly labels neurons in the dorsal and ventral cochlear nuclei. In the dorsal nuclei there is a peripheral punctate staining pattern in both cells and fibers, especially in the molecular layer. This region is also intensely stained by Timm histochemistry, a technique that detects zinc associated to glutamatergic terminals (Frederickson et al., 1988) Moreover, the molecular layer of the dorsal cochlear nucleus is an endpoint of numerous terminals coming from the auditory nerve, the intrinsic granule cells and other areas of the primary auditory pathway (Rubio and Juiz, 1998). It would be worthwhile to know what kind of functional relationship may exist between these neurochemical characteristics of the dorsal cochlear nuclei and the coincident MVa expression.

Zhao et al. (1996) demonstrated that another member of the myosin V class, the so-called myr 6 (myosin Vb), is specifically expressed in hippocampus, choroids plexus and amygdala of normal rats. Consequently, this paralogue may be a candidate to probe for the participation of brain myosins in temporal lobe hyperexcitable networks. In recent studies, an association between RING finger proteins and myosin V has been demonstrated (El-Husseini and Vincent, 1999; Ohkawa et al., 2001). Ohkawa et al. (2001) showed that the neural activity-related RING finger protein (NARF) was highly expressed in the hippocampus of mice treated with pentylenetetrazol, a potent convulsant. In addition, they demonstrated that treatment with the glutamate agonist, kainic acid, induced an up-regulation of the NARF mRNA and that this message was localized in neurites and growth cones and interacts with myosin V. NARF is also increased in the cerebellar Purkinje cells (Ohkawa et al., 2001) after seizures, a region where MVa labels extremely well. The MVa-NARF interaction seems to be necessary for maintenance of neural activity (Ohkawa et al., 2001). This is important not only for normal function such as enhanced neural activity present in long term potentiation, a correlate of learning, but in the case of pathological situations such as those found in epilepsy. In the same direction, it is interesting to note that neuronal and glial cytoskeleton associated proteins have been implicated in responses to traumatic, ischemic, excitotoxic lesions, mostly those present in epilepsy networks (Houser, 1999; Sloviter, 1999; Pollard et al., 1994; Represa and Ben-Ari, 1997).

The specific regional expression of brain proteins such as limbic associated membrane protein (Zacco et al., 1990), or the LYN protein, codified by a sarcoma proto-oncogene, *c-lyn* (Chen et al., 1996), indicates that our current regionally selective (e.g. cochlear nuclei; trapezoid body) MVa neural staining might be seen as an interesting marker of organized networks. For example it labels very strongly auditory, vestibular and somatosensory circuits. Additionally it labels sensory-motor and pure motor networks, for example brainstem motor nuclei, as well as basal ganglia, cerebellum and cortical circuitry. The idea that MVa can be considered as a regional specific brain marker is in consonance with other well-known types of brain markers such as the

Table 2. Regional patterns of MVa staining

Brain region	Staining pattern
Cortex	
Cingulate and retrosplenial	Mixed staining, generally punctated around cell bodies and fibers and with cell bodies stained denser in deeper layers
Frontal, forelimb and hindlimb areas, parietal (areas 1 and 2), insular and perirhinal	Generally, cortex was sparsely punctated in cell body, but deeper layers appeared densely stained
Piriform	Densely punctated in layer 2, sparsely in layer 3
Striatum	
Ventral pallidum	Punctate labeling in cell bodies and processes
Caudate putamen	Absent (in fact, extremely weak and homogeneous)
Amygdala	
Dorsolateral, ventrolateral, ventromedial and basolateral nuclei	Very sparse staining of cell bodies
Medial nucleus, posterodorsal area	Cell bodies peripherally punctated
Hippocampal formation	
Dentate gyrus, Ammon's horn and hilus	Almost absent, but isolated neurons in hilus and in CA had their cell bodies stained
Subiculum	Dense cell body staining
Thalamus	
Ventral posterolateral and medial nuclei	Dense cell body staining
Mediodorsal, posterior paraventricular, posterior group, laterodorsal and lateral posterior (mediodorsal area) nuclei	Cell body staining
Medial geniculate nucleus	Cell bodies densely stained
Hypothalamus	
Dorsomedial nucleus of hypothalamus	Cell bodies peripherally punctated
Median eminence	Dense cell body staining
Perifornical nucleus, medial tuberal nucleus, magnocellular nucleus of lateral hypothalamus, nubincertal nucleus, zona incerta	Cell body staining
Midbrain	
Superior colliculus	Variable staining, stronger in superficial gray layer and in intermediate gray layer
Posterior pretectal and deep mesencephalic nuclei	Cell bodies densely stained
Substantia nigra	Variable
Interpeduncular nucleus, red nucleus, Edinger-Westphal nucleus and lateral lemniscus	Cell bodies densely stained
Central gray	Cell bodies peripherally stained
Mesencephalic trigeminal nucleus	Mixed staining: cell bodies and peripheral staining
Inferior colliculus	Mixed: dense peripheral and cell bodies staining
Cerebellum	
Deep nuclei	Mixed: dense peripheral and cell bodies staining
Cerebellar cortex	Dense staining of Purkinje cells, a percentage of granular cells and molecular layer
Hindbrain	
Periolivary nucleus	Dense staining of both cell bodies and neuropila
Median raphe nucleus	Densely and sparsely punctated cell body staining
Pontine, oral pontine reticular, median raphe, paramedian raphe, raphe magnus and spinal trigeminal nuclei	Cell bodies densely stained
Cuneiform nucleus, prepositus hypoglossal nucleus and cochlear nucleus	Mixed: dense peripheral and cell bodies staining

Wisteria floribunda histochemistry, which labels the extracellular matrix, and is complementary to Nissl staining (Hilbig et al., 2001). Other marker is the parvalbumin immunohistochemistry, which specifically identifies GABA-positive interneurons, for example, in cortical Chandelier cells (DeFelipe, 1999).

The immunohistochemical studies presented here represent a comprehensive map of the regional and cellular distribution of MVa in the CNS of the adult rat and may contribute to the basic understanding of its role in brain function and plasticity, particularly related to phenomena that involve this molecular motor, such as neurite outgrowth, organelle transport and neurotransmitter-vesiclecycling. Moreover, the neurochemical characterization of MVa-positive cells and colocalization with other known markers may give clues toward cell function and specificity.

Acknowledgements—*To Rubens de Melo, Hildeberto Caldo and Domingos E. Pita for technical assistance. Thanks to Drs. Hernan Pimienta and Martha Escobar, from Universidad del Valle (Cali,*

Colombia), for their important help in the earlier phases of this work. To Dr. Norberto Cysne Coimbra and Dr. Enilza Maria Espreafico, for their valuable comments on a previous version of this manuscript. This work had financial support from: Fundação de-Amparo à Pesquisa do Estado de São Paulo (FAPESP), grants 93/3552–9, 99/06586–8 and 99/06756–0; Conselho Nacional de Desenvolvimento Científico e Tecnológico (CNPq), grant 521697/96–4; Programa para o Desenvolvimento de Núcleos de Excelência (PRONEX), grant 357/96 and Programa de Apoio ao Desenvolvimento Científico e Tecnológico (PADCT), grant 620099/95. Cristiane Queixa Tilelli was a holder of a pre-doctoral Fellowship from FAPESP (96/2445–2) and the South American Brain Research Organization (SABRO-IBRO). Norberto Garcia-Cairasco, Roy Edward Larson and Antonio Roberto Martins hold CNPq-Brazil Research fellowships.

REFERENCES

Chen S, Bing R, Rosenblum N, Hillman DE (1996) Immunohistochemical localization of Lyn (p56) protein in the adult rat brain. Neuroscience 71:89–100.

Cheney RE, O'Shea MK, Heuser JE, Coelho MV, Wolenski JS, Espreafico EM, Forscher P, Larson RE, Mooseker MS (1993) Brain myosin-V is a two-headed unconventional myosin with motor activity. Cell 75:13–23.

Coling DE, Espreafico EM, Kachar B (1997) Cellular distribution of myosin-V in the guinea pig cochlea. J Neurocytol 26:113–120.

Costa MCR, Mani F, Santoro W Jr, Espreafico EM, Larson RE (1999) Brain myosin-V, a calmodulin-carrying myosin, binds to calmodulin-dependent protein kinase II and activates its kinase activity. J Biol Chem 274:15811–15819.

DeFelipe J (1999) Chandelier cells and epilepsy. Brain 122:1807–1822.

Dekker-Ohno K, Hayasaka S, Takagishi Y, Oda S, Wakasugi N, Mikoshiba K, Inouye M, Yamamura H (1996) Endoplasmic reticulum is missing in dendritic spines of Purkinje cells of the ataxic mutant rat. Brain Res 714:226–230.

Drengk AC, Kajiwara JK, Garcia SB, Carmo VS, Larson RE, Zucoloto S, Espreafico EM (2000) Immunolocalisation of myosin-V in the enteric nervous system of the rat. J Anat Nerv Syst 78:109–112.

El-Husseini AE, Vincent SR (1999) Cloning and characterization of a novel RING finger protein that interacts with class V myosins. J Biol Chem 274:19771–19777.

Espíndola FS, Espreafico EM, Coelho MV, Martins AR, Costa FRC, Mooseker MS, Larson RE (1992) Biochemical and immunological characterization of p190-calmodulin complex from vertebrate brain: a novel calmodulin-binding myosin. J Cell Biol 118:359–368.

Espreafico EM, Cheney RE, Matteoli M, Nascimento AAC, De Camilli PV, Larson RE, Mooseker MS (1992) Primary structure and cellular localization of chicken brain myosin-V (p190), an unconventional myosin with calmodulim light chains. J Cell Biol 119:1541–1557.

Evans LL, Lee AJ, Brikgman PC, Mooseker MS (1998) Vesicle-associated brain myosin-V can be activated to catalyze actin-based transport. J Cell Sci 111:2055–2066.

Frederickson CJ, Howell GA, Haigh MD, Dansher G (1988) Zinc-containing fiber systems in the cochlear nuclei of the rat and mouse. Hear Res 36:203–212.

Futaki S, Takagishi Y, Hayashi Y, Ohmori S, Kanou Y, Inouye M, Oda S, Seo H, Iwaikawa Y, Murata Y (2000) Identification of a novel myosin-Va mutation in an ataxic mutant rat, dilute-opisthotonus. Mamm Genome 11:649–655.

Hasson T, Gillespie PG, Garcia JA, MacDonald RB, Zhao Y, Yee AG, Mooseker MS, Corey DP (1997) Unconventional myosins in inner-ear sensory epithelia. J Cell Biol 137:1287–1307.

Hilbig H, Bidmon H-J, Blohm U, Zilles K (2001) *Wisteria floribunda* agglutinin labeling patterns in the human cortex: a tool for revealing areal borders and subdivisions in parallel with immunocytochemistry. Anat Embryol 203:45–52.

Houser CR (1999) Neuronal loss and synaptic reorganization in temporal lobe epilepsy. Adv Neurol 79:743–761.

Laemmli UK, Favre M (1973) Maturation of the head of bacteriophage T4. J Mol Biol 80:575–599.

Langford GM, Molyneaux BJ (1998) Myosin V in the brain: mutations lead to neurological defects. Brain Res Rev 28:1–8.

Lowry OH, Rosebrough NJ, Farr AL, Randall RJ (1951) Protein measurement with the Folin phenol reagent. J Biol Chem 193:265–275.

Mani F, Espreafico EM, Larson RE (1994) Myosin-V is present in synaptosomes from rat cerebral cortex. Braz J Med Biol Res 27:2639–2643.

Martins AR, Dias MM, Vasconcelos TM, Caldo H, Costa MC, Chimelli L, Larson RE (1999) Microwave-stimulated recovery of myosin-V immunoreactivity from formalin-fixed, paraffin-embedded human CNS. J Neurosci Methods 92:25–29.

Mercer JA, Seperack PK, Strobel MC, Copeland NG, Jenkins NA (1991) Novel myosin heavy chain encoded by murine *dilute* coat colour locus. Nature 349:709–713.

Mooseker MS, Chency RE (1995) Unconventional myosins. Annu Rev Cell Dev Biol 11:633–675.

Nascimento AAC, Cheney RE, Tauhata SBF, Larson RE, Mooseker MS (1996) Enzymatic characterization and functional domain mapping of brain myosin-V. J Biol Chem 271:17561–17569.

Ohkawa N, Kokura K, Matsu-Ura T, Obinata T, Konishi Y, Tamura T (2001) Molecular cloning and characterization of neural activity-related RING finger protein (NARF): a new member of the RBCC family is a candidate for the partner of myosin V. J Neurochem 78:75–87.

Ohyama A, Komiya Y, Igarashi M (2001) Globular tail of myosin-V is bound to vamp-synaptobrevin. Biochem Biophys Res Commun 280:988–991.

Paxinos G, Watson C (1997) The rat brain in stereotoxic coordinates, 4th edn. London: Academic Press.

Pollard H, Khrestchatisky M, Moreaus J, Ben-Ary Y, Represa A (1994) Correlation between reactive sprouting and microtubule protein expression in epileptic hippocampus. Neuroscience 61:773–787.

Prekeris R, Terrian DM (1997) Brain myosin V is a synaptic vesicle-associated motor protein: evidence for a Ca^{2+}-dependent interaction with the synaptobrevin-synaptophisin complex. J Cell Biol 137:1589–1601.

Reck-Peterson SL, Provance DW Jr, Mooseker MS, Mercer JA (2000) Class V myosins. Biochem Biophys Acta 1496:36–51.

Represa A, Ben-Ari Y (1997) Molecular and cellular cascades in seizure-induced neosynapse formation. Adv Neurol 72:25–34.

Rosé, SD, Lejen, T, Casaletti, L, Larson, RE, Pene, TD, Trifaró, J-M (2003) Myosin Va, a chromaffin vesicle molecular motor involved in secretion. J Neurochem, in press.

Rubio ME, Juiz JM (1998) Chemical anatomy of excitatory endings in the dorsal cochlear nucleus of the rat: differential synaptic distribution of aspartate aminotransferase, glutamate, and vesicular zinc. J Comp Neurol 399:341–358.

Schlamp CL, Williams DS (1996) Myosin V in the retina: localization in the rod photoreceptor synapse. Exp Eye Res 63:613–619.

Schnell E, Nicoll RA (2001) Hippocampal synaptic transmission and plasticity are preserved in myosin Va mutant mice. J Neurophysiol 85:1498–1501.

Sloviter RS (1999) Status epilepticus-induced neuronal injury and network reorganization. Epilepsia 40 (Suppl 1):S34–39.

Tabb JS, Molyneaux BJ, Cohen DL, Kuznetsov SA, Langford GM (1998) Transport of ER vesicles on actin filaments in neurons by myosin V. J Cell Sci 111 (Pt 213221–3234.

Tauhata SBF, Vital dos Santos D, Taylor EW, Mooseker MS, Larson RE (2001) High affinity binding of brain myosin-Va to F-actin induced by calcium in the presence of ATP. J Biol Chem 276:39812–39818.

Towbin H, Staehelin T, Gordon J (1979) Electrophoretic transfer of proteins from polyacrylamide gels to nitrocellulose sheets: procedure and some applications. Proc Natl Acad Sci USA 76:4350–4354.

Zacco A, Cooper V, Chantler PD, Fisher-Hyland S, Horton HL, Levitt P

(1990) Isolation, biochemical characterization and ultrastructural analysis of the limbic system-associated membrane protein (LAMP), a protein expressed by neurons comprising functional neural circuits. J Neurosci 10:73–90.

Zhao L, Koslovsky JS, Reinhard J, Bähler M, Witt AE, Provance DW Jr, Mercer JA (1996) Cloning and characterization of myr 6, an unconventional myosin of the dilute/myosin-V family. Proc Natl Acad Sci USA 93:10826–10831.

(Accepted 9 July 2003)